

Development of the optical conductivity with doping in single-domain $\text{YBa}_2\text{Cu}_3\text{O}_{6+x}$

S. L. Cooper, A. L. Kotz, M. A. Karlow, M. V. Klein, W. C. Lee, J. Giapintzakis, and D. M. Ginsberg

Department of Physics, Materials Research Laboratory, University of Illinois at Urbana-Champaign, Urbana, Illinois 61801

(Received 5 September 1991; revised manuscript received 6 November 1991)

Optical studies of single-domain crystals of $\text{YBa}_2\text{Cu}_3\text{O}_{6+x}$ allow us to separate the CuO_2 -plane and CuO -chain contributions to the optical conductivity as a function of doping between 0.025 and 5.5 eV. We find several interesting consequences of doping on the optical conductivity of $\text{YBa}_2\text{Cu}_3\text{O}_{6+x}$: the 4.1-eV transition in tetragonal $\text{YBa}_2\text{Cu}_3\text{O}_{6.1}$ is split into a - and b -axis-polarized components by CuO -chain formation; oscillator strength associated with the charge-transfer band of insulating $\text{YBa}_2\text{Cu}_3\text{O}_{6.1}$ is redistributed to low frequencies; and the low-frequency conductivity in the CuO_2 planes evolves into a non-Drude response comprised of a single resolvable component. The CuO -chain conductivity, by contrast, is dominated by a midinfrared absorption band.

A number of unconventional properties of high- T_c compounds have been documented by optical studies, including the presence of a non-Drude low-frequency conductivity $\sigma(\omega)$ in metallic $\text{YBa}_2\text{Cu}_3\text{O}_{6+x}$,¹⁻³ and $\text{La}_{2-x}\text{Sr}_x\text{Cu}_2\text{O}_4$,⁴ and an anomalous redistribution of spectral weight with doping in 2:1:4 compounds such as $\text{La}_{2-x}\text{Sr}_x\text{Cu}_2\text{O}_4$,⁴ $\text{Nd}_{2-x}\text{Ce}_x\text{Cu}_2\text{O}_4$,⁴ and $\text{Pr}_{2-x}\text{Ce}_x\text{Cu}_2\text{O}_4$.⁵ Among the important questions these phenomena raise are the following: (1) Does the non-Drude response in the cuprates reflect the presence of more than one absorption band, or, rather, a single component of strongly interacting carriers; and (2) is the unusual spectral weight redistribution in the 2:1:4 compounds a universal consequence of doping in the cuprates? Unfortunately, CuO -chain contributions to the optical conductivity make it difficult to resolve these issues in studies of twinned $\text{YBa}_2\text{Cu}_3\text{O}_{6+x}$.

In this paper we report reflectivity and ellipsometry measurements of single-domain $\text{YBa}_2\text{Cu}_3\text{O}_{6+x}$, which allow us to isolate the development of the CuO_2 plane conductivity as a function of doping. We find a number of interesting consequences of doping in $\text{YBa}_2\text{Cu}_3\text{O}_{6+x}$, including a splitting of the 4.1-eV excitation in tetragonal $\text{YBa}_2\text{Cu}_3\text{O}_{6.1}$ into a - and b -axis-polarized components, a redistribution of the spectral weight above the charge-transfer band in $\text{YBa}_2\text{Cu}_3\text{O}_{6.1}$ to low energies, and the appearance of a non-Drude low-frequency conductivity in the CuO_2 planes that is comprised of a single resolvable component.

Optical reflectivity and ellipsometry studies were performed on single-domain samples of $\text{YBa}_2\text{Cu}_3\text{O}_{6+x}$ with $x \sim 0.1$, $x \sim 0.6$ ($T_c = 66$ K), and $x \sim 1$ ($T_c = 90$ K). The samples were grown using a method described elsewhere.^{6,7} Optical reflectivity spectra from 0.025 to 5.5 eV were obtained in a near-normal incidence configuration with a rapid scanning interferometer. The different sources, polarizers, and detectors used in these studies provided substantial spectral overlap, and the different spectral ranges covered had reflectivity mismatches of less than 1%. In order to accurately determine the conductivities and other optical parameters from our reflectivity data, we used ellipsometry spectra on the same samples to correct errors that result from extrapolating the reflectivity in a standard Kramers-Kronig analysis.⁸ The ellip-

sometric measurements were obtained between 1.5 and 5.5 eV using a technique detailed elsewhere.⁹ Our correction procedure is similar to that described recently by Bozovic,¹⁰ and it involves first selecting a reflectivity extrapolation so that the phase estimated from the Kramers-Kronig analysis, $\Theta_{\text{KK}}(\omega)$, provides the best possible overlap with the "exact" phase determined from ellipsometry measurements, $\Theta_{\text{ellip}}(\omega)$. $\Theta_{\text{KK}}(\omega)$ is then forced to equal $\Theta_{\text{ellip}}(\omega)$ above roughly 3 eV in order to correct any remaining errors at high frequencies. Finally, the optical constants between 0.025 and 5 eV are determined from the measured $R(\omega)$ and the corrected $\Theta_{\text{KK}}(\omega)$ using standard constitutive relations.⁸ The optical constants determined between 0.025 and 5 eV in this fashion merge smoothly into the exact ellipsometric values between 2 and 5 eV [see the top curve of Fig. 2(a)], and are therefore expected to be accurate to within experimental error.

Figure 1 illustrates the normal-state reflectivity spectra of single-domain $\text{YBa}_2\text{Cu}_3\text{O}_{6+x}$ for several values of x , and for incident light polarized along the a (solid lines) and b axis (dashed lines). Our room-temperature reflectivity results for single-domain $\text{YBa}_2\text{Cu}_3\text{O}_7$ are comparable to those observed by Schlesinger *et al.*,³ and are slightly higher than those obtained by Koch, Geserich, and Wolf¹¹ and Petrov *et al.*¹² In Fig. 2, the a -axis and b -axis normal-state conductivities of single-domain $\text{YBa}_2\text{Cu}_3\text{O}_{6+x}$ have been obtained from our reflectivity spectra using the correction procedure described above. The conductivity of insulating $\text{YBa}_2\text{Cu}_3\text{O}_{6.1}$ [top curve, Fig. 2(a)] exhibits an absorption gap below 1.5 eV and sharp peaks near 1.75 and 4.1 eV. The 1.75-eV peak has an analog in all the cuprates,^{13,14} and has been associated with transitions across the O $2p$ -Cu $3d$ charge-transfer gap.^{4,5,13,14} The 4.1-eV peak, however, is specific to $\text{YBa}_2\text{Cu}_3\text{O}_{6+x}$ and has been variously attributed to Cu(1)-O(4) transitions,¹⁵ excitations in the Ba-O(4) planes,¹⁶ and intraionic excitations on the Cu(1) site.¹⁷ Upon doping from $\text{YBa}_2\text{Cu}_3\text{O}_{6.1}$ to orthorhombic $\text{YBa}_2\text{Cu}_3\text{O}_{6.6}$, a metallic low-frequency conductivity develops in both a and b directions, spectral weight in the conductivity between 1.5 and 3 eV diminishes, and the 4.1-eV peak weakens and appears to split into a - and b -axis-polarized components near 4.1 and 4.7 eV, respectively.

While the loss of spectral weight in the 4.1-eV transi-

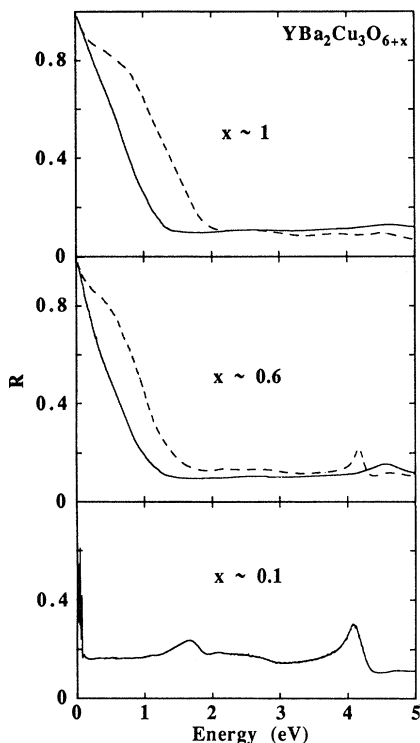


FIG. 1. Room-temperature reflectivity vs frequency for single-domain $\text{YBa}_2\text{Cu}_3\text{O}_{6+x}$, with $x \sim 0.1$ (lower curve), $x \sim 0.6$ ($T_c = 66$ K) (middle curves), and $x \sim 1$ ($T_c = 90$ K) (top curves). For data on orthorhombic samples (middle and top curves), the solid lines are the reflectivities obtained with incident light along the a axis, $E_i \parallel a$, while the dashed lines are obtained with $E_i \parallel b$.

tion and the appearance of a 4.7-eV feature with doping have been observed in previous ellipsometric studies of twinned samples,^{15–17} the lack of polarization information has hampered a definitive assignment of these excitations. Our results illustrate that the 4.1-eV excitation becomes strongly polarized along the b direction upon placing oxygen into chain sites, supporting the attribution, by Kircher *et al.*, of this feature to $3d_{3z^2-1}$ to $4p_{x,y}$ transitions on the Cu(1) site.¹⁷ Ba-O(4)-plane transitions,¹⁶ by contrast, should be less sensitive to the addition of oxygen into the chains, while Cu(1)-O(4) excitations¹⁵ should be predominantly c axis polarized. Furthermore, the appearance of an additional a -axis-polarized feature at intermediate doping suggests that a degeneracy associated with the initial or final state of the 4.1-eV transition is lifted by CuO-chain formation. A possible candidate is the degenerate $4p_{x,y}$ final state in the interpretation of Kircher *et al.*, since the presence of regular lengths of CuO chains should strongly affect the $4p_x$ band between the X and M points of the Brillouin zone, while leaving the $4p_y$ band between Y and M relatively undisturbed.⁹

The conductivity associated with the charge-transfer band (1.5–3 eV) is also quite sensitive to doping, exhibiting a substantial loss of oscillator strength through the metal-insulator transition. This behavior can be more quantitatively illustrated by examining the integrated spectral weight in the conductivity between 0 and ω ,

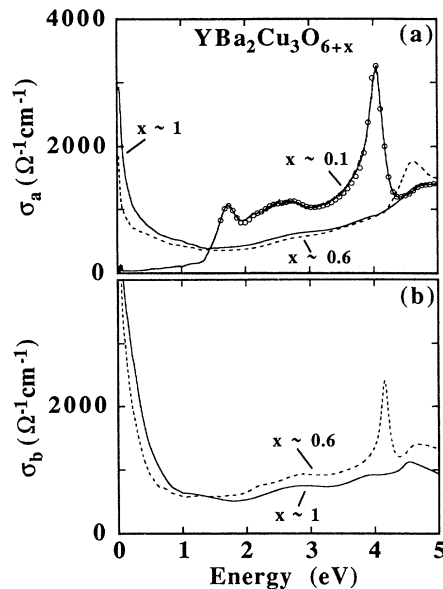


FIG. 2. Room-temperature conductivity vs frequency along (a) the a axis ($=\text{CuO}$ planes) ($E_i \parallel a$), and (b) the b axis ($E_i \parallel b$), for $x \sim 0.1$, $x \sim 0.6$ ($T_c = 66$ K), and $x \sim 1$ ($T_c = 90$ K). In (a), the open circles on the top curve ($x \sim 0.1$) show the conductivity determined directly from ellipsometry measurements.

defined as²

$$N_{\text{eff}}(\omega) = \frac{2mV}{\pi e^2} \int \sigma(\omega') d\omega', \quad (1)$$

where $N_{\text{eff}}(\omega)$ (m/m^*) is the effective number of carriers per unit cell contributing to the conductivity below ω , m and e are the bare electron mass and charge, respectively, m^* is the effective electron mass, and V is the unit-cell volume. Figure 3 illustrates the development of the integrated spectral weights in the a -axis conductivities [Fig. 2(a)] as a function of frequency. The integrated spectral weight in insulating $\text{YBa}_2\text{Cu}_3\text{O}_{6.1}$ remains near zero through the conductivity gap [see Fig. 2(a)], but begins to attain appreciable values above the charge-transfer absorption edge. In the metallic phase ($x \geq 0.6$), the integrated spectral weight exhibits a rapid rise at low frequencies, reflecting the presence of a Drude-like band formed by the dopants. Yet in spite of the additional dopant contribution at $x \sim 0.6$, the integrated spectral weight curves for $\text{YBa}_2\text{Cu}_3\text{O}_{6.1}$ and $\text{YBa}_2\text{Cu}_3\text{O}_{6.6}$ intersect near 3 eV. This result implies that doping between $x = 0.1$ and 0.6 does not affect the *total* spectral weight in the CuO₂-plane conductivity below 3 eV, but rather causes a *redistribution* of weight from the charge-transfer band region (1.5–3 eV) to lower frequencies ($\omega \leq 1.5$ eV). The redistribution of spectral weight in $\text{YBa}_2\text{Cu}_3\text{O}_{6+x}$ is similar to that observed in the 2:1:4 compounds,^{4,5} and it reflects a reconstruction of the high-energy electronic states in the CuO₂ planes with doping. Notably, the deleterious effect of doping on the charge-transfer band is inconsistent with a simple single-electron picture of Cu-O charge transfer in the cuprates. Rather, there appear to be many-body contributions to the fundamental absorption band in the cuprates that are strongly

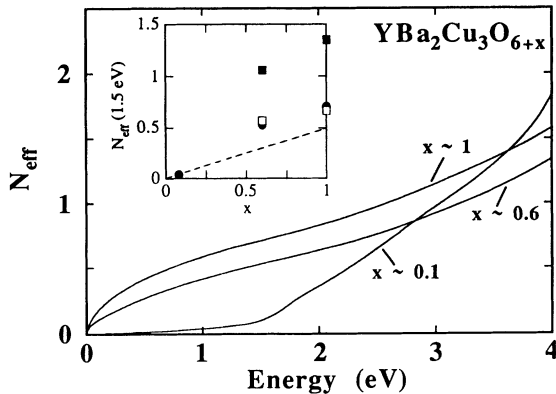


FIG. 3. Integrated spectral weight vs frequency for the a -axis conductivities in Fig. 2(a), obtained using Eq. (1). The inset summarizes the spectral weights integrated to $\omega = 1.5$ eV for the b axis (solid squares), a axis (=CuO₂ plane) (solid circles), and chain [= $\sigma_b(\omega) - \sigma_a(\omega)$] (open squares) contributions to the conductivity. The dashed line is the estimated doping contribution to the CuO₂ planes, $N_{\text{eff}} = 0.5x$, assuming the effective mass equals the free-electron mass.

affected by the addition of carriers.

In view of the redistribution of high-frequency states with doping in YBa₂Cu₃O_{6+x}, it is important to examine to what extent the growth of spectral weight below the absorption gap ($\omega \leq 1.5$ eV) originates from dopant contributions or from weight transferred from above the charge-transfer band. This is examined in the inset of Fig. 3, which compares the integrated spectral weight below the absorption edge [$N_{\text{eff}}(\omega = 1.5$ eV)] as a function of doping for b -axis (solid squares), a -axis (=CuO₂ plane) (solid circles), and CuO-chain (= $\sigma_b - \sigma_a$) (open squares) contributions. A comparison of chain and plane contributions for $x \geq 0.6$ illustrates that the low-frequency spectral weight in the metallic phases is evenly divided between the planes and chains. Assuming equivalent effective masses on the chains and planes, therefore, we estimate that 50% of the holes introduced by doping go onto the CuO₂ planes in metallic YBa₂Cu₃O_{6+x}, with the balance going onto the CuO chains. Significantly, the integrated CuO₂-plane spectral weight below $\omega = 1.5$ eV exceeds that attributable to doping alone, $N_{\text{eff}} = 0.5x$ (dashed line, inset), suggesting that additional spectral weight must arise by transferring weight from the charge-transfer band to low frequencies. This result corroborates reports of similar behavior in 2:1:4 compounds.^{4,5}

Perhaps the most interesting feature of the normal-state optical response in the cuprates is the non-Drude low-frequency conductivity, which has been alternatively ascribed to frequency-dependent scattering of a single electronic component,^{3,4,18–21} and two-component absorption involving intraband and interband transitions.^{22,23} Unfortunately, identifying the optical response associated with the CuO₂ planes in twinned YBa₂Cu₃O_{6+x} is difficult because of CuO-chain contributions to the conductivity. In Fig. 4(a), we isolate the low-frequency CuO₂-plane conductivity (σ_a) as a function of doping in single-domain YBa₂Cu₃O_{6+x} (solid lines). Also shown for comparison are the CuO-chain ($\sigma_b - \sigma_a$) contributions for $x \sim 0.6$

and $x \sim 1$ (dotted lines). Our study illustrates that for $x \geq 0.6$, the chain conductivity exhibits both Drude and midinfrared components, while the CuO₂-plane conductivity appears to exhibit a single-component response that falls off much more slowly than a standard Drude term ($\sim \omega^{-2}$). These results corroborate and extend to lower doping earlier studies of single-domain YBa₂Cu₃O₇.³ Notably, the absence of a distinguishable secondary absorption in the a -axis conductivity of moderately doped YBa₂Cu₃O_{6+x} places stronger limitations on the possibility of two-component absorption in the CuO₂ planes of YBa₂Cu₃O_{6+x}. It is also interesting that the absence of a resolvable secondary band in the CuO₂ plane conductivity of YBa₂Cu₃O_{6.6} is in contrast to the large midinfrared band observed at intermediate doping in several 2:1:4 compounds.^{4,5} This discrepancy suggests that the 2:1:4 compounds transit more slowly than YBa₂Cu₃O_{6+x} between a low-density metallic regime, in which impurity²⁴ or other secondary absorption processes⁴ can be substantial, and a high-density metallic regime characterized by a single low-frequency contribution.^{4,24}

Evidence that the a -axis conductivity below 1 eV is comprised of a single component [Fig. 4(a)] also suggests that the non-Drude CuO₂-plane conductivity in doped YBa₂Cu₃O_{6+x} ($x \geq 0.6$) may arise from frequency-dependent scattering of the carriers.^{3,18} In this case, the a -axis conductivities are more appropriately described by a generalized Drude model,²⁵

$$\sigma(\omega) = \frac{\omega_p^2/4\pi}{[m^*(\omega)/m][\tau^{*-1}(\omega) - i\omega]}, \quad (2)$$

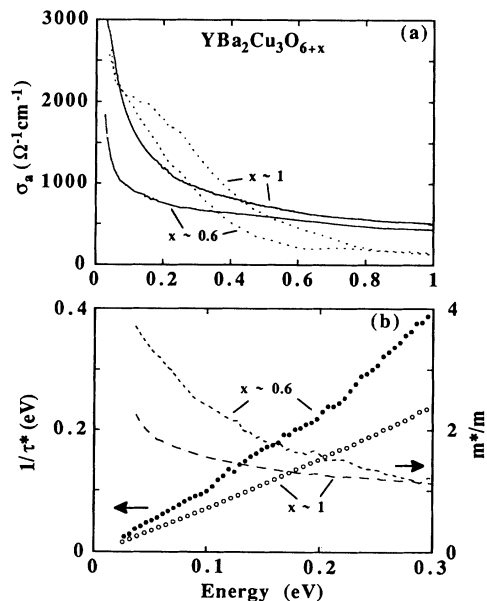


FIG. 4. (a) Room-temperature a -axis conductivity vs frequency in single-domain YBa₂Cu₃O_{6+x} for $x \sim 0.6$ ($T_c = 66$ K) and $x \sim 1$ ($T_c = 90$ K) (solid lines). The dotted line compares the chain contributions to the conductivity, $\sigma_b(\omega) - \sigma_a(\omega)$, for $x \sim 0.6$ and 1; (b) renormalized scattering rate $1/\tau^*(\omega)$ (open and solid circles) and effective-mass enhancement $m^*(\omega)/m$ (dashed lines), derived from the measured complex conductivity $\sigma(\omega)$ using Eq. (2). At each value of x , ω_p^2 is obtained using the value of N_{eff} at $\omega = 1.5$ eV.

where $m^*(\omega)/m$ is the effective-mass enhancement, and $1/\tau^*(\omega) = 1/\tau(\omega)[m/m^*(\omega)]$ is the renormalized scattering rate. Figure 4(b) illustrates the effective-mass enhancements $m^*(\omega)/m$ and renormalized scattering rates $1/\tau^*(\omega)$ obtained from the *a*-axis conductivities in Fig. 4(a). The effective-mass enhancement in the CuO_2 planes is found to decrease from 4 to 2 upon doping from $x \sim 0.6$ to $x \sim 1$. Furthermore, the renormalized scattering rate is linear in frequency throughout much of the metallic phase, $1/\tau^*(\omega) \propto \omega$, with a slope that decreases with doping from 1.33 at $x \sim 0.6$ to 0.75 at $x \sim 1$. As noted previously for $\text{YBa}_2\text{Cu}_3\text{O}_7$,³ the linear frequency dependence of $1/\tau^*(\omega)$ in $\text{YBa}_2\text{Cu}_3\text{O}_{6+x}$ is consistent with various models of the strongly correlated normal state in which the imaginary part of the quasiparticle self-energy scales linearly with energy, $\text{Im}\Sigma(\omega) \propto \omega$.^{20,21,26} However, the frequency-dependent scattering analysis in Fig. 4(b) also indicates an increase in the slope of $1/\tau^*(\omega)$ with decreased doping, reflecting an *increased* quasiparticle coupling at low doping. This result is not obviously consistent with any of the above models, although a better assessment of this issue must await a more detailed theoretical treatment of doping effects.

In summary, we have studied the development of the optical conductivity in single-domain crystals of $\text{YBa}_2\text{Cu}_3\text{O}_{6+x}$ as a function of x . We find evidence that the

4.1-eV transition in $\text{YBa}_2\text{Cu}_3\text{O}_6$ evolves into *a*- and *b*-axis-polarized components at intermediate doping. This behavior is attributed to the splitting of a degenerate band in $\text{YBa}_2\text{Cu}_3\text{O}_{6.1}$ upon forming CuO chains. We also find that the CuO_2 planes evolve with doping by transferring spectral weight from the charge-transfer band region (1.5–3 eV) to low frequencies, in agreement with earlier results in 2:1:4 compounds. Unlike these earlier studies, however, we find no evidence for an intrinsic midinfrared band in the low-frequency optical conductivity of the CuO_2 planes. Rather, by separating the CuO -chain and plane contributions to the low-frequency optical conductivity for $x \geq 0.6$, we conclude that the chains are dominated by a midinfrared absorption band, while the planes exhibit a single-component, non-Drude response. We analyze the latter response with a frequency-dependent scattering model, and find a linear in frequency scattering rate that decreases in slope with increased doping.

This work was supported by the National Science Foundation (Grant No. DMR 88-09854) through the Science and Technology Center for Superconductivity and in part by the U.S. Department of Energy, Basic Energy Sciences–Materials Science Division under Contract No. W-31-109-Eng-38. One of us (M.A.K.) acknowledges support from the Department of Defense.

- ¹For a review, see T. Timusk and D. B. Tanner, in *Physical Properties of High Temperature Superconductors I*, edited by D. M. Ginsberg (World Scientific, Singapore, 1989), p. 339.
- ²J. Orenstein, G. A. Thomas, A. J. Millis, S. L. Cooper, D. H. Rapkine, T. Timusk, L. F. Schneemeyer, and J. V. Waszczak, *Phys. Rev. B* **42**, 6342 (1990).
- ³Z. Schlesinger, R. T. Collins, F. Holtzberg, C. Feild, S. H. Blanton, U. Welp, G. W. Crabtree, and Y. Fang, *Phys. Rev. Lett.* **65**, 801 (1990).
- ⁴S. Uchida, T. Ido, H. Takagi, T. Arima, Y. Tokura, and S. Tajima, *Phys. Rev. B* **43**, 7942 (1991).
- ⁵S. L. Cooper, G. A. Thomas, J. Orenstein, D. H. Rapkine, A. J. Millis, S.-W. Cheong, A. S. Cooper, and Z. Fisk, *Phys. Rev. B* **41**, 11 605 (1990).
- ⁶J. P. Rice and D. M. Ginsberg, *J. Cryst. Growth* **109**, 432 (1991).
- ⁷W. C. Lee and D. M. Ginsberg, *Phys. Rev. B* **44**, 2815 (1991).
- ⁸F. Stern, *Solid State Physics* (Academic, New York, 1963), Vol. 15.
- ⁹A. L. Kotz, M. V. Klein, W. C. Lee, J. Giapintzakis, D. M. Ginsberg, and B. W. Veal (unpublished).
- ¹⁰I. Bozovic, *Phys. Rev. B* **42**, 1969 (1990).
- ¹¹B. Koch, H. P. Geserich, and Th. Wolf, *Solid State Commun.* **71**, 495 (1989).
- ¹²M. P. Petrov, A. I. Grachev, M. V. Krasin'kova, A. A. Nechitailov, V. V. Poborchii, S. I. Shagin, and S. V. Miridonov, *Pis'ma Zh. Eksp. Teor. Fiz.* **50**, 25 (1989) [*JETP Lett.* **50**, 29 (1989)].
- ¹³Y. Tokura, H. Takagi, T. Arima, S. Koshihara, T. Ido, S. Ishibashi, and S. Uchida, *Physica C* **162–164**, 1231 (1989).
- ¹⁴S. L. Cooper, G. A. Thomas, A. J. Millis, P. E. Sulewski, J.

Orenstein, D. H. Rapkine, S.-W. Cheong, and P. L. Trevor, *Phys. Rev. B* **42**, 10785 (1990).

- ¹⁵M. K. Kelly, P. Barboux, J.-M. Tarascon, D. E. Aspnes, W. A. Bonner, and P. A. Morris, *Phys. Rev. B* **38**, 870 (1988).
- ¹⁶M. Garriga, J. Humlicek, M. Cardona, and E. Schonherr, *Solid State Commun.* **66**, 1231 (1988).
- ¹⁷J. Kircher, M. K. Kelly, S. Rashkeev, M. Alouani, D. Fuchs, and M. Cardona, *Phys. Rev. B* **44**, 217 (1991).
- ¹⁸G. A. Thomas, J. Orenstein, D. H. Rapkine, M. Capizzi, A. J. Millis, L. F. Schneemeyer, and J. V. Waszczak, *Phys. Rev. Lett.* **61**, 1313 (1988).
- ¹⁹R. T. Collins, Z. Schlesinger, F. Holtzberg, P. Chaudhari, and C. Feild, *Phys. Rev. B* **39**, 6571 (1989).
- ²⁰C. M. Varma, P. B. Littlewood, S. Schmitt-Rink, E. Abrahams, and A. E. Ruckenstein, *Phys. Rev. Lett.* **63**, 1996 (1989).
- ²¹J. Ruvalds and A. Virostek (unpublished).
- ²²K. Kamaras, S. L. Herr, C. D. Porter, N. Tache, D. B. Tanner, S. Etamad, T. Venkatesan, E. Chase, A. Inam, X. D. Wu, M. S. Hegde, and B. Dutta, *Phys. Rev. Lett.* **64**, 84 (1990).
- ²³T. Timusk, S. L. Herr, K. Kamaras, C. D. Porter, D. B. Tanner, D. A. Bonn, J. D. Garrett, C. V. Stager, J. E. Greedan, and M. Reedyk, *Phys. Rev. B* **38**, 6683 (1988).
- ²⁴G. A. Thomas, in *Proceedings of the Scottish Universities Summer School on the Physics of High Temperature Superconductors*, St. Andrews, edited by D. Tunstall (in press).
- ²⁵J. W. Allen and J. C. Mikkelsen, *Phys. Rev. B* **15**, 2952 (1977).
- ²⁶P. W. Anderson, in *Strong Correlation and Superconductivity*, edited by H. Fukuyama, S. Maekawa, and A. Malozamoff (Springer-Verlag, Berlin, 1989), p. 2.